Bioorganic & Medicinal Chemistry Letters 20 (2010) 6581–6586

Contents lists available at ScienceDirect

Bioorganic & Medicinal Chemistry Letters

journal homepage: www.elsevier.com/locate/bmcl

Optimization of a series of dipeptides with a P3 threonine residue as non-covalent inhibitors of the chymotrypsin-like activity of the human 20S proteasome

Christopher Blackburn *, Cynthia Barrett, Jonathan L. Blank, Frank J. Bruzzese, Nancy Bump, Lawrence R. Dick, Paul Fleming, Khristofer Garcia, Paul Hales, Zhigen Hu, Matthew Jones, Jane X. Liu, Darshan S. Sappal, Michael D. Sintchak, Christopher Tsu, Kenneth M. Gigstad

Millennium Pharmaceuticals Inc., 40 Landsdowne St., Cambridge, MA 02139, United States

ARTICLE INFO

Article history:
Received 13 August 2010
Accepted 7 September 2010
Available online 15 September 2010

Keywords:
Proteasome
Non-covalent inhibitor

ABSTRACT

Starting from a tripeptide screening hit, a series of dipeptide inhibitors of the proteasome with Thr as the P3 residue has been optimized with the aid of crystal structures in complex with the β-5/6 active site of y20S. Derivative **25**, (β5 IC_{50} = 7.4 nM) inhibits only the chymotryptic activity of the proteasome, shows cellular activity against targets in the UPS, and inhibits proliferation.

Inhibition of the 20S core particle of the proteasome, which leads to the accumulation of substrate proteins involved in gene expression, signal transduction, cell cycle control and apoptosis, is preferentially cytotoxic to cancer cells.[1–3] Indeed, inhibition of the proteasome is a clinically effective anti-cancer therapy, primarily for hematological malignancies.[4,5] The active sites of the 20S core particle located on the β1, β2, and β5 sub-units are classified as caspase-like, trypsin-like, and chymotrypsin-like, respectively[1–3] and induce proteolysis of peptide substrates via the hydroxyl nucleophile of the N-terminal threonine residues ($Thr1O^{\gamma}$).[6,7] Various natural and synthetic inhibitors have been described[8–10] that form covalent adducts with the active site threonine hydroxyls. These include peptide aldehydes and vinyl sulfones,[2] α′β′-epoxyketones (such as Carfilzomib, Fig. 1),[11] 2-keto-1,3,4-oxadiazoles,[12] β-lactones[13] (Salinosporamide A, and Omuralide, for example), β-lactams[14,15] and boronic acids.[16] The dipeptide boronic acid bortezomib (**1**) (PS-341 or VELCADE®) is used clinically to treat multiple myeloma and refractory mantle cell lymphoma, and is being evaluated for the treatment of other malignancies.[17] Bortezomib is a high affinity slowly reversible inhibitor (K_i = 0.55 nM; dissociation $t_{1/2}$ ca. 110 min)[10] of the β5 site of the proteasome[7] (and to a lesser extent the β1 and β2 sites) the adduct of which with the N-terminal threonine of 20S has been characterized by X-ray crystallography.[18] Two additional boronic acids MLN9708[10,19] and CEP-18870[20] are undergoing clinical trials.

Non-covalent inhibitors of the catalytic β sub-units of the 20S core particle may offer therapeutic advantages such as more widespread tissue distribution due to their more rapid dissociation kinetics. The few non-covalent inhibitors reported to date include TMC-95A (Fig. 2), a cyclic peptide natural product that competitively inhibits the chymotrypsin-like activity of the proteasome with nanomolar potency[21] as well as synthetic analogs of moderate potency[22] and linear analogs such as **2**.[23] A related trimethoxy-L-phenylalanine-containing tripeptide, **3**, optimized[24,25] from a statine-like HTS hit,[26] has been shown to inhibit the chymotrypsin-like activity reversibly with an IC_{50} of 15 nM and a binding mode proposed.[27] In addition, a series of 5-methoxy-1-indanone capped dipeptides (e.g., CVT-659)[28] has been reported; although these compounds were designed to be covalent, our recent X-ray data with an analogous compound[29,30] suggest that N-terminal indanones do not form covalent adducts with the 20S proteasome. Recently, we described in detail the biological properties of a tripeptide screening hit **4**;[30] this compound shows comparable potency to bortezomib but is a rapid-equilibrium inhibitor of the β5 (chymotrypsin-like) activity of the constitutive proteasome and does not inhibit the activity of either the β1 or β2 sites. Compound **4** also inhibits TNFα-induced activation of NFκB-Luc in HEK293 cells consistent with potent proteasome inhibition and is cytotoxic toward human cancer cell lines. We further showed that although dipeptide analog **5** has considerably lower enzymatic and cellular activities, improvements to these non-covalent inhibitors can be effected by variation of the P1 through P4 residues.[29,30] In this Letter we discuss the SAR of a sub-series of dipeptide derivatives

* Corresponding author. Tel.: +1 617 761 6811.
E-mail addresses: blackburn@mpi.com, chris.blackburn@mpi.com (C. Blackburn).

0960-894X/$ - see front matter © 2010 Elsevier Ltd. All rights reserved.
doi:10.1016/j.bmcl.2010.09.032

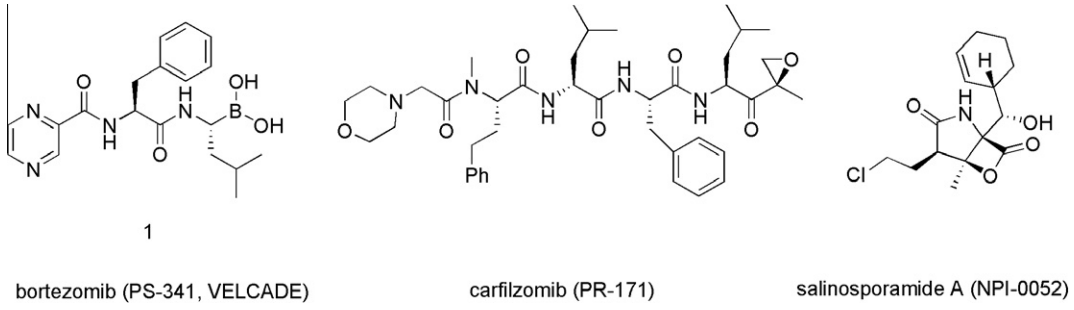

Figure 1. Covalent proteasome inhibitors.

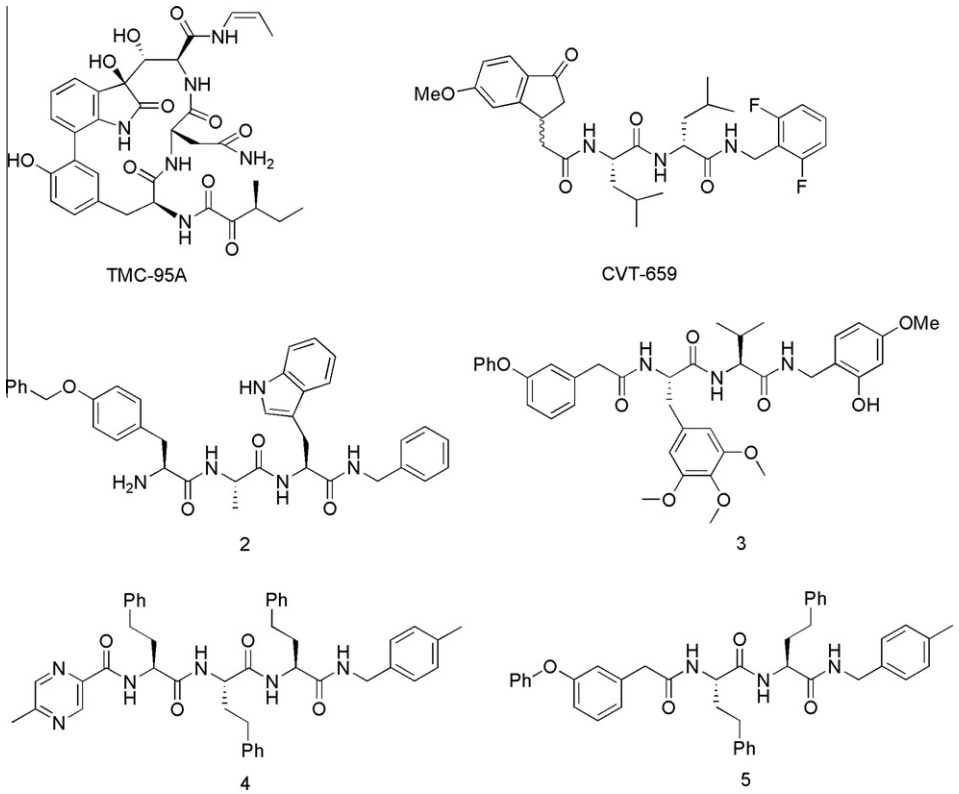

Figure 2. Non-covalent proteasome inhibitors.

focusing on analogs with threonine residues at the P3 position and report the crystal structures of representative examples in complex with yeast 20S.

Results and discussion. We approached the optimization of compound **5** by systematically modifying the C-terminal cap (P1 residue), central amino acids (P2, P3) and N-terminal cap (P4) in a series of compound libraries.[29] In our first series of compounds, we retained 4-methylbenzylamine and 3-phenoxyphenylacetyl[27] at the termini while varying the amino acids in an attempt to find replacements for the hydrophobic homo-phenylalanine (hPhe) residues. Compounds were prepared using automated liquid-phase peptide synthesis methods employing Boc-protection of the *N*-α-amino groups as described in detail previously.[30] Thus, for example, 4-methylbenzylamine was coupled to the appropriate Boc-*N*-α-amino acid in the presence of HBTU. After removal of the Boc protecting group under acidic conditions, the next protected α-amino acid was coupled, de-protected and capped at the N-terminus (Scheme 1).[31]

The inhibitory activities of these analogs on the rate of hydrolysis of the β5 substrate Ac-WLA-AMC by human 20S constitutive proteasome were determined. Proteasomal degradation of the inhibitory protein IκBα, (following its phosphorylation and ubiquitination) activates the NFκB transcription factor in cells in response to TNFα stimulation.[28,30,32] Thus, monitoring the effect of proteasome inhibitors on the NFκB pathway was used to assess cellular activity. In addition, the long-term effects of these compounds on cell viability were assessed in the human lung cancer cell line Calu6 by monitoring cellular ATP levels. Testing over one hundred analogs of compound **5** from the first library did not lead to any derivatives where *both* h-Phe residues had been replaced that showed comparable activity to **5**. However, we did identify *O*-methyl serine (**6**) and threonine (**7**) derivatives (Fig. 3) that exhibited twofold improvements in inhibitory activity compared to **5** (Table 1) and considerably improved solubilities[33] albeit with modest cellular activities (NFκB assay).

In the next series of compound libraries, prepared similarly, we scanned for alternatives to 3-phenoxyphenylacetyl as the N-terminal cap (P4 residue) and noted that analogs **8** and **9**, derived from an isomeric benzoic acid, showed significant improvements in enzymatic activity accompanied by sub-μM potencies in the

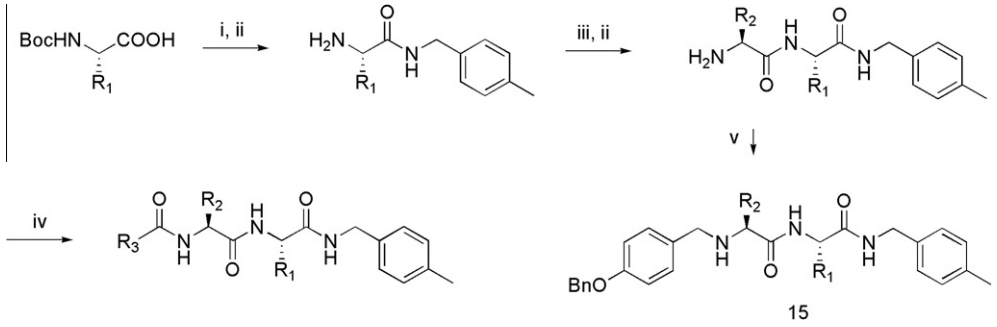

Scheme 1. Reagents and conditions: (i) $ArCH_2NH_2$, HBTU, NMM, DMF, 25 °C, 24 h; (ii) 4 N HCl, dioxane, 25 °C, 8 h; (iii) $BocNHCH(R_2)COOH$, HBTU, NMM, DMF, 25 °C, 24 h; (iv) R_3COOH, HBTU, NMM, DMF, 25 °C, 24 h; (v) *p*-$BnOC_6H_4CHO$, $NaBH_3CN$, MeOH, 25 °C, 24 h.

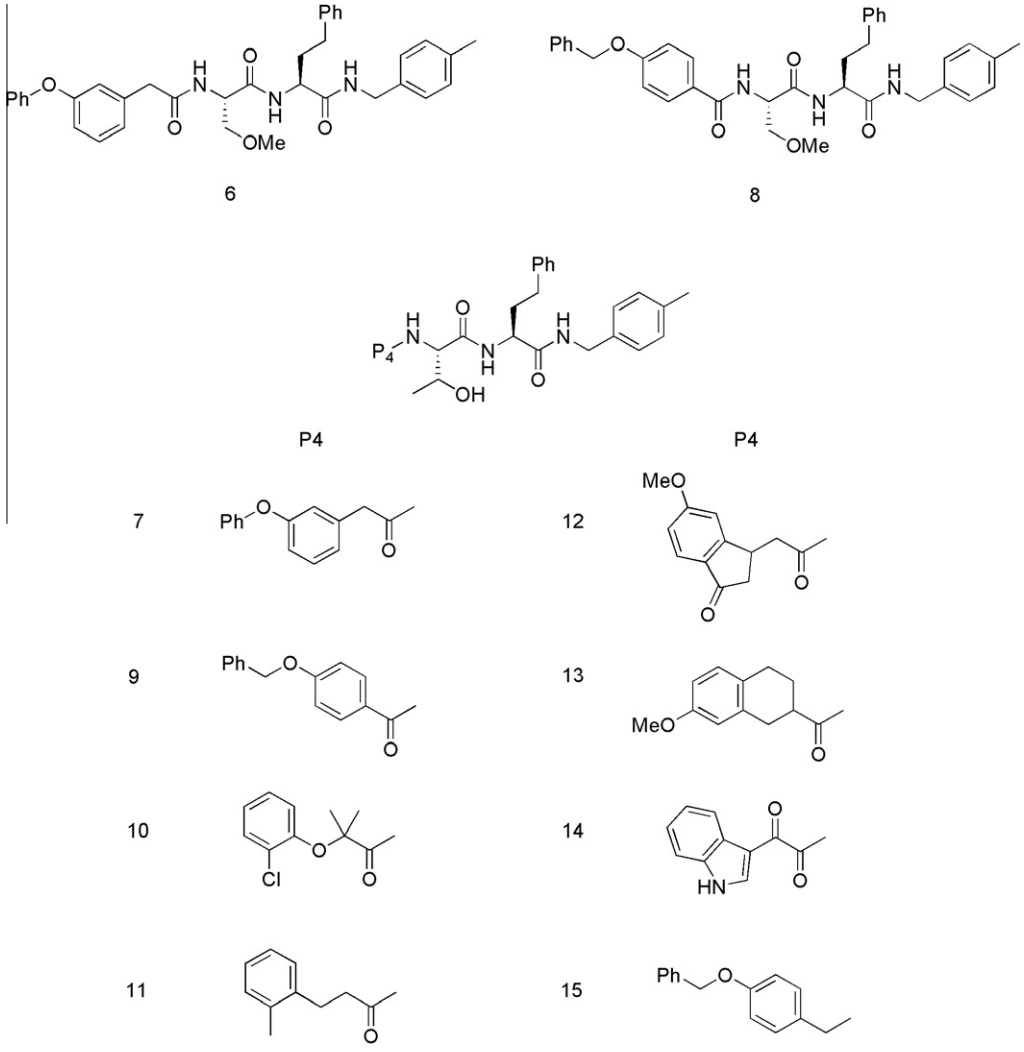

Figure 3. Structures of human 20S inhibitors **6**–**15**.

cellular assays. Threonine derivatives were generally superior to their *O*-methylserine counterparts so these derivatives were selected for further optimization at P4. A diverse selection of hydrophobic acyl residues was tolerated at this position as illustrated by the β5 inhibitory activities, cellular activities (NFκB assay) and anti-proliferative effects of analogs **10–14** (Table 1). β-Ketoamide **14** is particularly noteworthy with a comparable profile to **4**. Compound **15**, however, with a methylene replacement for the P4 carbonyl of compound **9** was over 100-fold less potent. Modifications to the P1 residue such as methylation at *N*-1 (compound **16**) or the benzylic position (compound **17**) abolished activity (Fig. 4). Likewise, extending the benzyl P1 residue by an additional methylene group was also detrimental; compound **18**, for example, has little activity. Several smaller residues were incorporated at the P1 site such as ethyl and allyl (analogs **19** and **20**, respectively), leading to >10-fold reductions in potency. Removal of the 4′-methyl group from the P1 benzyl residue also led to a slight reduction in potency (compare **21** with **9**). While introduction of a chlorine atom at the

Table 1
Enzymatic, cellular and anti-proliferative effects of a series of capped dipeptides compared to bortezomib

Compound	Human[a] 20S-PA28 IC_{50} (nM) β5c	HEK293 NFκB-Luc IC_{50} (nM) (% max inh)[b]	Cell viability[c] Calu6 LC_{50} (nM)
1	8.2	10 (100)	6.1
4	16	47 (79)	140
5	1100	>50,000 (28)	>25,000
6	550	6100 (40)	>25,000
7	450	24,000 (30)	15,000
8	74	340 (78)	220
9	20	120 (81)	380
10	75	690 (97)	1500
11	120	690 (80)	2300
12	25	320 (89)	1200
13	20	95 (89)	2300
14	7.3	90 (100)	136
15	3100	>50,000 (37)	14,000
16	9100	4400 (86)	6600
17	>100,000	>50,000	9000
18	3200	>50,000	>25,000
19	440	2600 (98)	5100
20	100	880 (99)	2800
21	68	710 (68)	1400
22	210	15,000 (44)	>25,000
23	13	29 (87)	290
24	31	330 (71)	2700
25	7.4	28 (81)	110

[a] Purified human erythrocyte 20S (0.25 nM) was used as a source of constitutive (c) proteasome to measure the peptidase activity of the β5 (chymotrypsin-like) sub-site. The assay was performed in the presence of 15 μM of the fluorogenic substrate Ac-WLA-AMC, 12 nM PA28α, and a titration of each inhibitor.

[b] Inhibition of NFκB-luciferase activity in HEK293 cells was determined by pre-incubation of the cells (10,000 per well) with compound for 1 h followed by stimulation with 10 ng/ml TNF-α in the continued presence of compound for 3 h. The IC_{50} and percentage inhibition of NFκB-luciferase activity are given.

[c] Effects of compounds on the viability of Calu6 cells (2000 per well) were assessed following incubation with compound for 72 h. Viability was assessed by monitoring cellular ATP levels using the luminescence-based ATPlite assay as described previously.[30] In each case, results are mean values of at least three independent experiments.

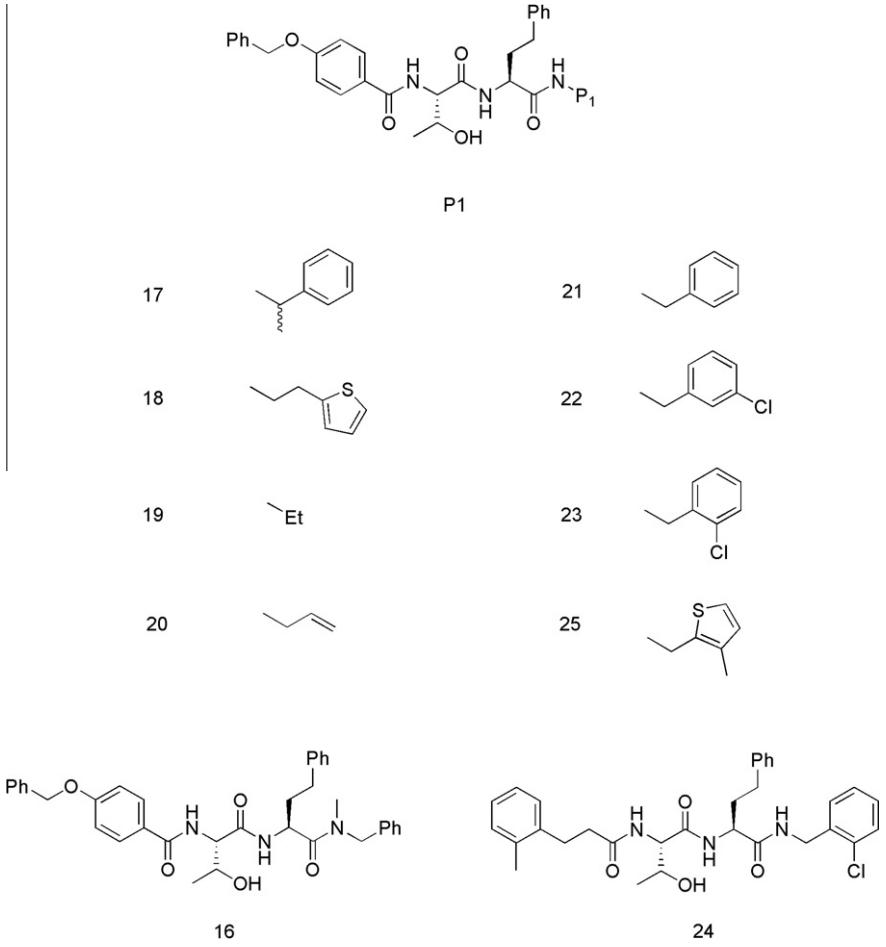

Figure 4. Structures of human 20S inhibitors **16**–**25**.

meta-position of the benzylic P1 residue, as in compound **22**, was unfavorable, *ortho*-chlorobenzyl derivatives **23** and **24** and *ortho*-methylthiophene derivative **25** showed high inhibitory activities in enzymatic and cellular assays.

Many of the SAR trends noted above can be explained from X-ray structures of the inhibitors in complex with the β5 site of yeast open gate 20S.[34] To date, we have solved 30 such structures[29] and reported four of these in the open literature.[30] The co-crystals of compounds **24** and **25**, obtained at 2.6 and 2.85 Å resolution, respectively[35] have not been reported previously and their important features are illustrated in Figures 5–7. The same general binding mode that we reported earlier[30] involving β-sheet-type H-bonding interactions was observed (Fig. 5). These backbone interactions include H-bonding between the amide flanked by the P1 and P2 residues and Thr21 and Gly47 of the β5 site accounting for the loss of activity of N-methylated derivative **16**. As shown in Figure 6, a benzylic residue can fit tightly into the S1 binding pocket and diminished hydrophobic interactions accounts for the lower potency of the allyl and ethyl derivatives **19** and **20**. Additional hydrophobic interactions with sub-pockets within S1 are observed for the 4′-methyl compounds;[30] for example, compound **9** is threefold more potent than unsubstituted analog **21**. Similarly, *ortho*-substituents on a P1 benzyl residue can access an additional sub-pocket contributing to the high potencies of chloro-compounds **23** and **24** and *ortho*-methyl thiophene **25** (Fig. 6). The π-system of the hPhe residue of these compounds forms a ledge interaction with Gly47-Gly48 within the shallow S2 binding pocket that we have discussed previously,[30] while the threonine residue partially occupies the well defined S3 specificity pocket. In contrast, the S4 pocket is very large and ill-defined accounting for the wide range of hydrophobic substituents tolerated at this position.

The reduced activity of the secondary amine capped analog **15** can be attributed to a weaker hydrogen bonding interaction between the nitrogen and Asp-114 compared to its analog **9** or a less optimal projection of the benzyl group toward the P4 pocket. The value of the 4-benzyloxybenzoyl P4 residue appears to be associated with an induced fit effect (Fig. 7). Thus, in comparison to compound **24**, where the P4 residue partially occupies the S4 binding pocket, the benzyloxybenzoyl group of **25** projects farther into the binding pocket accessing additional interactions with Pro94 and Tyr96 in the adjacent β-6 site. By forcing apart Tyr5 and

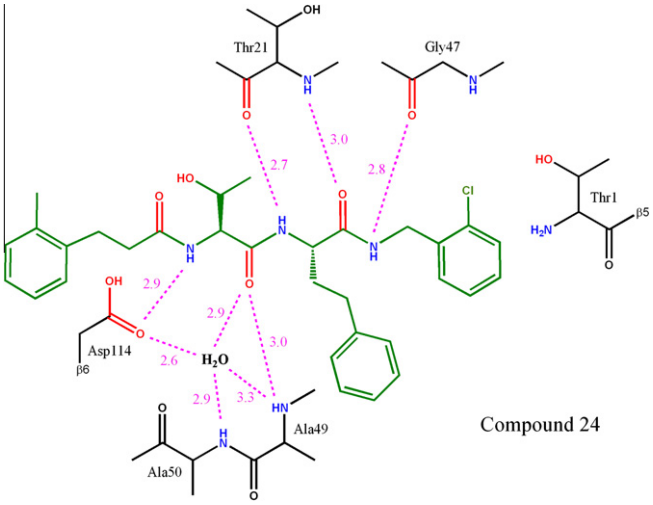

Figure 5. Schematic representation of the β5/β6 active site of 20S with compound **24** bound. Key hydrogen bonds between the inhibitor and the protein are shown as dashed lines colored magenta, with distances indicated in Angstroms.

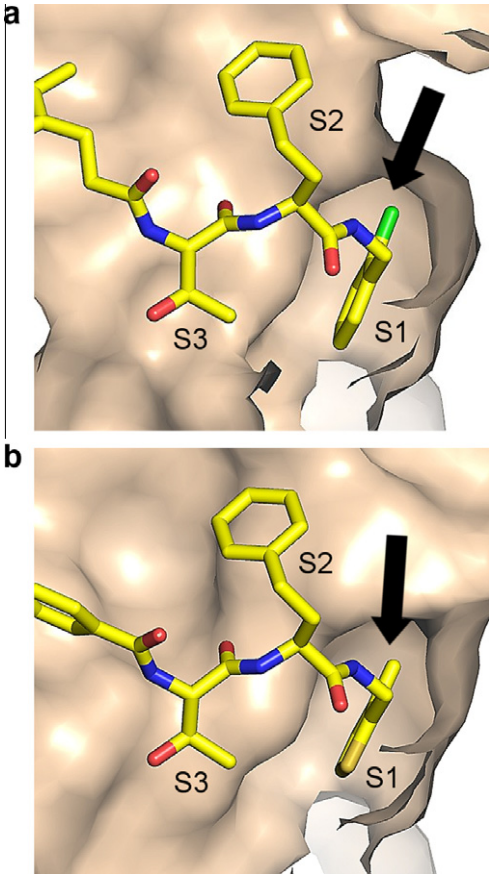

Figure 6. Molecular surface of the 20S β5 site showing the S1 sub-pocket being filled by the *ortho*-chloro substituent in P1 for compound **24** (left panel), compared to the *ortho*-methyl substituent for compound **25** (right panel). Atoms are shown in ball-and-stick representation with carbon in yellow, nitrogen in blue, oxygen in red, chlorine in green, and sulfur in orange. Figure made using PyMOL Molecular Graphics System (DeLano Scientific, Palo Alto, CA).

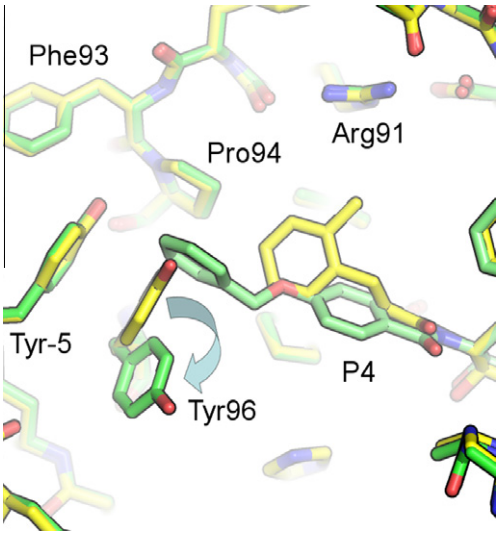

Figure 7. Superposition of the structures for compounds **24** and **25** bound to the β5/β6 active site of 20S highlighting the S4 pocket and changes in the position of Tyr96. All residues labeled are from the β6 sub-unit. Coloring scheme is as described above, with carbon atoms for the compound **24** structure shown in two shades of yellow and for the compound **25** structure in two shades of green.

Tyr96 the latter can form a σ–π edge interaction with the P4 aryl group of compound **25**.

In general, we observed a good correlation between the inhibitory IC_{50} values for 20S β5 activity in vitro and NFκB-Luc activity in cells, with four of the analogs (**13**, **14**, **23**, and **25**) showing comparable cellular potencies to those of tripeptide **4**. It should be noted that all the analogs described here are highly selective inhibitors of the β5 sub-unit with no significant inhibitory activity (IC_{50} >20 μM) of human β1 and β2 sub-units. In addition, representative examples showed only modest inhibitory activity at a concentration of 100 μM for ten unrelated proteases.[36] The cytotoxic LC_{50} values of these compounds in Calu6 cells also correlate with their 20S β5 potencies, indicating that selective inhibition of the chymotrypsin-like site of the proteasome is sufficient to inhibit cell proliferation. Although none of the compounds were as potent as bortezomib, five examples gave cytotoxicity LC_{50} values below 500 nM and compound **25**, with an LC_{50} of 95 nM, showed superior activity to that of **4** (Table 1) tracking the NFκB-Luc activity in HEK293 cells. These data further support the notion that selective non-covalent inhibition of the β5 (chymotrypsin-like) site of the proteasome is sufficient to inhibit the degradation of TNFα-dependent NFκB activity and the proliferation of cancer cells. Several compounds reported here have comparable or greater potencies than any previously reported non-covalent inhibitor. In addition, co-crystals of compounds **24** and **25** bound to the β5 active site of yeast 20S unequivocally demonstrate the binding mode of this series of compounds and providing further opportunities for optimization.

Acknowledgements

We are grateful to Drs. Marion Schmidt and Dan Finley for providing the yeast 20S expression strains and to Dr. Juan Gutierrez and Zhi Li their assistance with preparation of the yeast 20S enzymes. We gratefully acknowledge the analytical chemistry assistance of David Lok and Nina Molchanova.

Supplementary data

Supplementary data associated with this article can be found, in the online version, at doi:10.1016/j.bmcl.2010.09.032.

References and notes

1. (a) Hochstrasser, M. *Curr. Opin. Cell Biol.* **1995**, *7*, 215; (b) Hershko, A.; Ciechanover, A. *Ann. Rev. Biochem.* **1998**, *67*, 425; (c) Goldberg, A. L. *Biochem. Soc. Trans.* **2007**, *35*, 12.
2. Kisselev, A. F.; Goldberg, A. L. *Chem. Biol.* **2001**, *8*, 739.
3. Borissenko, L.; Groll, M. *Chem. Rev.* **2007**, *107*, 687.
4. Adams, J.; Palombella, V. J.; Sausville, E. A.; Johnson, J.; Destree, A.; Lazarus, D. D.; Maas, J.; Pien, C. S.; Prakash, S.; Elliott, P. J. *Cancer Res.* **1999**, *59*, 2615.
5. Orlowski, R. Z.; Kuhn, D. J. *Clin. Cancer Res.* **2008**, *14*, 1649.
6. Loewe, J.; Stock, D.; Jap, B.; Zwickl, P.; Baumeister, W.; Huber, R. *Science* **1995**, *268*, 533.
7. Groll, M.; Ditzel, S.; Lowe, J.; Stock, D.; Bochtler, M.; Bartunik, H. D.; Huber, R. *Nature* **1997**, *386*, 463.
8. García-Echeverria, C. *Int. J. Pept. Res. Ther.* **2006**, *12*, 49.
9. Groll, M.; Huber, R.; Moroder, L. *J. Pept. Sci.* **2009**, *15*, 58.
10. Dick, L. R.; Fleming, P. E. *Drug Discovery Today* **2010**, *15*, 243.
11. (a) Meng, L.; Mohan, R.; Kwok, B. H. B.; Eloffson, M.; Sin, N.; Crews, C. M. *Proc. Natl. Acad. Sci. U.S.A.* **1999**, *96*, 10403; (b) Kuhn, D. J.; Chen, Q.; Voorhees, P. M.; Strader, J. S.; Shenk, K. D.; Sun, C. M.; Demo, S. D.; Bennett, M. K.; van Leeuwen, F. W. B.; Chanan-Khan, A. A.; Orlowski, R. Z. *Blood* **2007**, *110*, 3281; (c) Groll, M.; Kim, K. B.; Kairies, N.; Huber, R.; Crews, C. M. *J. Am. Chem. Soc.* **2000**, *122*, 1237.
12. Rydzewski, R. M.; Burrill, M.; Mendonca, R.; Palmer, J. T.; Rice, M.; Tahilramani, R.; Bass, K. E.; Leung, L.; Gjerstad, E.; Janc, J. W.; Pan, L. *J. Med. Chem.* **2006**, *49*, 2953.
13. (a) Feling, R. H.; Buchanan, G. O.; Mincer, T. J.; Kauffman, C. A.; Jensen, P. R.; Fenical, W. *Angew. Chem., Int. Ed.* **2003**, *42*, 355; (b) Reddy, L. R.; Fournier, J.-F.; Reddy, B. V. S.; Corey, E. J. *Org. Lett.* **2005**, *7*, 2699; (c) Chauhan, D.; Catley, L.; Li, G.; Podar, K.; Hideshima, T.; Velankar, M.; Mitsiades, C.; Mitsiades, N.; Yasui, H.; Letai, A.; Ovaa, H.; Berkers, C.; Nicholson, B.; Chao, T.-H.; Neuteboom, S. T. C.; Richardson, P.; Palladino, M. A.; Anderson, K. C. *Cancer Cell* **2005**, *8*, 407; (d) Groll, M.; Huber, R.; Potts, B. C. M. *J. Am. Chem. Soc.* **2006**, *128*, 5136.
14. Hogan, P. C.; Corey, E. J. *J. Am. Chem. Soc.* **2005**, *127*, 15386.
15. Imbach, P.; Lang, M.; Garcıa-Echeverrıa, C.; Guagnano, V.; Noorani, M.; Roesel, J.; Bitsch, F.; Rihs, G.; Furet, P. *Bioorg. Med. Chem. Lett.* **2007**, *17*, 358.
16. Adams, J.; Behnke, M.; Chen, S.; Cruickshank, A. A.; Dick, L. R.; Grenier, L.; Klunder, J. M.; Ma, Y.-T.; Plamondon, L.; Stein, R. L. *Bioorg. Med. Chem. Lett.* **1998**, *8*, 333.
17. (a) Richardson, P. G.; Mitsiades, C.; Schlossman, R.; Ghobrial, I.; Hideshima, T.; Munshi, N.; Anderson, K. C. *Expert Rev. Anticancer Ther.* **2008**, *8*, 1053; (b) O'Connor, O. A.; Czuczman, M. S. *Leuk Lymphoma* **2008**, *49*, 59; (c) Hideshima, T.; Richardson, P.; Chauhan, D.; Palombella, V. J.; Elliott, P. J.; Adams, J.; Anderson, K. C. *Cancer Res.* **2001**, *61*, 3071; (d) Williamson, M. J.; Blank, J. L.; Bruzzese, F. J.; Cao, Y.; Daniels, J. S.; Dick, L. R.; Labutti, J.; Mazzola, A. M.; Patil, A. D.; Reimer, C. L.; Solomon, M. S.; Stirling, M.; Tian, Y.; Tsu, C. A.; Weatherhead, G. S.; Zhang, J. X.; Rolfe, M. *Mol. Cancer Ther.* **2006**, *5*, 3052; (e) Richardson, P. G.; Barlogie, B.; Berenson, J.; Singhal, S.; Jagannath, S.; Irwin, D.; Rajkumar, S. V.; Srkalovic, G.; Alsina, M.; Alexanian, R.; Siegel, D.; Orlowski, R. Z.; Kuter, D.; Limentani, S. A.; Lee, S.; Hideshima, T.; Esseltine, D.-L.; Kauffman, M.; Adams, J.; Shenkein, D. P.; Anderson, K. C. *N. Eng. J. Med.* **2003**, *348*, 2609.
18. Groll, M.; Berkers, C. R.; Ploegh, H. L.; Ovaa, H. *Structure* **2006**, *14*, 451.
19. Kupperman, E.; Lee, E. C.; Cao, Y.; Bannerman, B.; Fitzgerald, M.; Berger, A.; Yu, J.; Yu, Y.; Bruzzese, F.; Liu, J.; Blank, J.; Garica, K.; Tsu, C.; Dick, L.; Fleming, P.; Yu, L.; Manfredi, M.; Rolfe, M.; Bolen, J. *Cancer Res.* **2010**, *70*, 1970.
20. Piva, R.; Ruggeri, B.; Williams, M.; Costa, G.; Tamagno, I.; Ferrero, D.; Giai, V.; Coscia, M.; Peola, S.; Massaia, M.; Pezzoni, G.; Allievi, C.; Pescalli, N.; Cassin, M.; di Giovine, S.; Nicoli, P.; de Feudis, P.; Strepponi, I.; Roata, I.; Ferrancini, R.; Bussolati, B.; Camussi, G.; Jones-Bolin, S.; Hunter, K.; Zhao, H.; Neri, A.; Palumbo, A.; Berkers, C.; Huib, O.; Bernareggi, A.; Inghirami, G. *Blood* **2008**, *111*, 2765.
21. (a) Koguchi, Y.; Kohno, J.; Nishio, M.; Takahashi, K.; Okuda, T.; Ohnuki, T.; Komatsubara, S. J. *Antibiotics (Tokyo)* **2000**, *53*, 105; (b) Groll, M.; Koguchi, Y.; Huber, R.; Kohno, J. *J. Mol. Biol.* **2002**, *311*, 543.
22. Groll, M.; Gotz, M.; Kaiser, M.; Weyher, E.; Moroder, L. *Chem. Biol.* **2006**, *13*, 607.
23. Basse, N.; Piguek, S.; Papapostolou, D.; Ferrier-Berthelot, A.; Richey, N.; Pagano, M.; Sarthou, P.; Sobczak-Thepot, J.; Reboud-Ravaux, M.; Vidal, J. *J. Med. Chem.* **2007**, *50*, 2842.
24. García-Echeverría, C.; Imbach, P.; France, D.; Furst, P.; Lang, M.; Noorani, M.; Scholz, D.; Zimmermann, J.; Furet, P. *Bioorg. Med. Chem. Lett.* **2001**, *11*, 1317.
25. Furet, P.; Imbach, P.; Furst, P.; Lang, M.; Noorani, M.; Zimmermann, J.; Garcia-Echeverria, C. *Bioorg. Med. Chem. Lett.* **2001**, *11*, 1321.
26. Furet, P.; Imbach, P.; Furst, P.; Lang, M.; Noorani, M.; Zimmermann, J.; Garcia-Echeverria, C. *Bioorg. Med. Chem. Lett.* **2002**, *12*, 1331.
27. Furet, P.; Imbach, P.; Noorani, M.; Koeppler, J.; Laumen, K.; Lang, M.; Guagnano, V.; Fuerst, P.; Roesel, J.; Garcia-Echeverria, C. *J. Med. Chem.* **2004**, *47*, 4810.
28. (a) Lum, R. T.; Kerwar, S. S.; Meyer, S. M.; Nelson, M. G.; Schow, S. R.; Shiffman, D.; Wick, M. M.; Joy, A. *Biochem. Pharmacol.* **1998**, *55*, 1391; (b) Lum, R. T.; Nelson, M. G.; Joly, A.; Horsma, A. G.; Lee, G.; Meyer, S. M.; Wick, M. M.; Schow, S. R. *Bioorg. Med. Chem. Lett.* **1998**, *8*, 209.
29. Blackburn, C.; Achab, A.; Blank, J.; Bump, N.; Bruzzese, F.; Dick, L.; Fleming, P.; Garcia, K.; Gigstad, K.; Hales, P.; Herman, L.; Jones, M.; Li, Z.; Liu, J.; Mishechkina, A.; Nagayoshi, M.; Sappal, D.; Sintchak, M.; Tsu, C. *Abstracts, 36th Northeast Regional Meeting of the American Chemical Society*, Hartford, CT, United States, October 7–10, NERM-055, 2009.
30. Blackburn, C.; Gigstad, K.; Hales, P.; Garcia, K.; Jones, M.; Bruzzese, F.; Barrett, C.; Liu, J.; Soucy, T.; Sappal, D.; Bump, N.; Olhava, E.; Fleming, P.; Dick, L. R.; Tsu, C.; Sintchak, M.; Blank, J. L. *Biochem. J.* **2010**, *430*, 461.
31. All final compounds were purified by preparative reverse phase HPLC using mass-directed fraction collection conducted on an Agilent 1100 series LC/MSD instrument using a Waters SunFire C18 5 μm Prep OBD column (19 × 150 mm). The compounds were eluted with a water–MeCN gradient (0.1% formic acid) optimized by the A2Prep Agilent software. All compounds described herein were further characterized by ^{1}H NMR spectroscopy and high resolution mass spectrometry.
32. Palombella, V. J.; Rando, O. J.; Goldberg, A. L.; Maniatis, T. *Cell* **1994**, *78*, 773.
33. Representative turbidometric solubilities were obtained by sequential dilutions of 10 mM DMSO stock solutions into 50 mM potassium phosphate buffer at pH 6.8. Measurements were made on a Labsystems Nepheloskan Ascent plate reader equipped with a quartz halogen lamp emitting between 580 and 630 nm giving the following solubility results: **4**: 6 μM; **5**; 3 μM; **6**: 50 μM; **7**: 50 μM; **8**: 50 μM; **9**: 25 μM; **10**: 12 μM; **11**: 50 μM; **12**: 100 μM.
34. Given the close correlation in potencies of proteasome inhibitors from various classes for the human and yeast 20S enzymes,[30] we are confident optimizing compounds for human 20S inhibitory activity based on X-ray structures obtained with yeast 20S.
35. Co-crystals of the y20S proteasome with inhibitors **24** and **25** were solved with resolutions of 2.85 Å and 2.5 Å, respectively (see Supplementary data).
36. Protease selectivity was assessed by testing the inhibitory activities of representative compounds on a panel of purified human enzymes including cathepsin B and L, coagulation factor β-XIIa, chymotrypsin, elastase, plasmin, thrombin, tissue plasminogen activator, trypsin and calpain I.